Journal of the Meteorological Society of Japan, Vol. 76, No. 1, pp. 57–71, 1998

Climatological Aspects and Mechanism of Spring Persistent Rains over Central China

By Shao-Fen Tian[1]

Environmental Research Center, University of Tsukuba, 305 Japan

and

Tetsuzo Yasunari

Institute of Geoscience, University of Tsukuba, 305 Japan

(Manuscript received 10 December 1996, in revised form 12 November 1997)

Abstract

In this study we examine the large-scale atmospheric circulation associated with the spring persistent rains (SPR) over Central China in March and April based on the climatological means and we propose a physical explanation of this rainy season.

Low-level southwesterlies to the south of the middle and lower reaches of the Yangtze River (southern China) are responsible for SPR. Low-level southwesterlies are identified over southern China on the climatological mean wind field in SPR, and the appearance of the southwesterlies at the end of February is consistent with the onset of SPR. The southerlies, which are limited to southern China, the Indochina Peninsula and the South China Sea, are important for moisture transport to Central China and the moisture convergence there.

Seasonal evolutions of low-level temperature, geopotential height and wind fields suggest that the low-level southerlies over southern China, the Indochina Peninsula and the South China Sea in SPR are caused by the westward pressure gradient associated with the eastward temperature gradient around the region from the Indochina Peninsula to the western North Pacific to east of the Philippines. The southerlies are the geostrophic winds associated with the westward pressure gradient. The eastward temperature/westward pressure gradients are most evident in March and April, and they are a result of the time-lag in the seasonal warming between the Indochina Peninsula and the western North Pacific to east of the Philippines. In addition, the coincidences of spatial distributions and seasonal evolutions from February through May between the low-level temperature and the surface sensible heat flux (SHF) suggest that the differential heating due to SHF between the two regions is likely responsible for the east-west thermal contrast.

Much higher correlations than the 99 % significance level among the year to year fluctuations of SPR, the eastward temperature/westward pressure gradients over the region from the Indochina Peninsula to the western North Pacific to east of the Philippines are identified. The close relationship between SPR and the eastward temperature/westward pressure gradients on both the seasonal and interannual bases strongly suggests that the east-west thermal contrast in spring between the Indochina Peninsula and the western North Pacific to the east of the Philippines plays the primary role in SPR formation.

1. Introduction

It is well known in China that Central China experiences another pronounced rainy period besides Meiyu or *the Plum rain* period in early summer — the spring persistent rains (SPR). SPR is particularly evident between the middle and lower reaches of the Yangtze River and the Nanling mountains (roughly 25–30°N), and occurs most frequently in March and April (Bao, 1987).

The rain-belt or axis of maximum rainfall over East China shows a great seasonal variation. It stays between the Yangtze River and the Nanling mountains from mid October to early May (Kao and Hsu, 1962), then retreats southward to South China in mid May to cause the pre-monsoon rainy

1 Corresponding author address: S.-F. Tian, Environmental Research Center, University of Tsukuba, 1-1-1 Tennodai, Tsukuba, Ibaraki, 305, Japan. E-mail: tian@etesia.geo.tsukuba.ac.jp

(PMR) period there (Xu *et al.*, 1983; Guo, 1985). In summer, it experiences three stagnant periods and two northward shifts (Kao and Hsu, 1962; Xu *et al.*, 1983; Guo, 1985). The three stagnant periods correspond to PMR period in South China, Meiyu season in Central China and the summer monsoon rainy period in North China, respectively. The two northward abrupt shifts correspond to the onsets of Meiyu over Central China in mid June and the summer monsoon rainy period over North China in mid July. Although the rain-belt changes little in its location between mid October and early May, the rainfall is much greater in spring than in winter, which corresponds to SPR in Central China.

The seasonal variation of the rain-belt over East China is closely related to the Asian monsoon activities, and considerable climatological studies have been done on the seasonal advance associated with the Asian summer monsoon. Most researchers (*e.g.*, Dao and Chen, 1957; Yeh *et al.*, 1959; Yoshino, 1965, 1966) regarded the onset of Meiyu as the beginning of the Asian summer monsoon. Dao and Chen (1957) found that the nearly simultaneous onsets of Meiyu in Central China, Baiu in Japan and the Indian summer monsoon in mid June are closely related to the northward movement and weakening of the upper westerly jet stream[1] over East Asia. Based on the abrupt meridional movement of the upper westerly jet over East Asia, Yeh *et al.* (1959) concluded that there are only two natural seasons: summer and winter. They also stated that winter is considerably long but transitional seasons are negligibly short. Yoshino (1965, 1966) divided early summer (May to July) into four stages based on the locations of the surface frontal zones and the regimes of the 500 hPa westerlies over East Asia, and concluded that the atmospheric circulation in the first stage (late May through early June) is basically the winter monsoon circulation regime.

The rain-belt over East China before the onset of Meiyu is generally considered to be associated with the winter monsoon circulation, and to be related to the upper westerly jet stream (*e.g.*, Kao and Hsu, 1962; Yoshino, 1965, 1966; Kato, 1989). From the thermal wind relation, the upper westerly jet is located in the latitudes where the strongest vertical wind shear and the maximum meridional temperature gradient exist. Actually, a relatively strong meridional temperature gradient or baroclinity exists around Central China until early May (Kato, 1985, 1987, 1989; Kato and Kodama, 1992; Hirasawa *et al.*, 1995). In other words, SPR is a phenomenon within the mid-latitude baroclinic zone and associated with the polar front over the eastern coast of the continent. In this sense, the statement that SPR is related to the upper westerly jet is not wrong. However, it can not explain the inconsistency that the much stronger upper westerly jet or baroclinity yields much smaller rainfall in winter, but the much weaker jet or baroclinity brings much greater rainfall in SPR.

On day to day synoptic charts, when the spring rainy weather occurs, the lower- and middle-tropospheric southwesterlies on the western flank of the anticyclone over the Philippines and the northwesterlies to the west of the trough in the mid-latitudes of East Asia confluence over the middle and lower reaches of the Yangtze River to form the stationary front there (Bao, 1987).

However, few climatological studies have focussed on the atmospheric circulation associated with SPR. Climatological aspects of SPR is only mentioned in some studies of seasonal division of China. In a research of seasonal division of China, Hsu and Kao (1962) mentioned that the rainfall over Central China increases markedly, and the subtropical high of the western North Pacific around the Philippines appears in early March. Their result implied indirectly a possible linkage between SPR and the subtropical high over the western North Pacific around the Philippines. However, it is not clear what a large-scale atmospheric circulation in spring is responsible for SPR. There has been no a satisfactory physical explanation for the existence of SPR.

Recently, Matsumoto (1989, 1990, 1992) successfully detected several abrupt seasonal changes in convective activities and wind fields over the global tropics, and the Asian and Australian monsoon regions in spring, though SPR was not mentioned in his studies. However, it remains unknown how SPR is related to his abrupt seasonal changes in the large-scale atmospheric indices.

The purpose of this study is to examine the climatological characteristics of the large-scale atmo-

1 Two types of upper westerly jet streams are distinguished: subtropical westerly jet stream and polar front westerly jet stream. The former is formed mainly due to the dynamical process or the convergence of angular momentum from both the tropics and the mid-latitudes. It is strongest at around 200 hPa level and only accompanies a large meridional temperature gradient in the upper troposphere. On the other hand, the latter is formed mainly due to the thermal effect or the meridional temperature gradients in the lower and especially middle troposphere, which is associated with the polar front. From the thermal wind relation a strong vertical wind shear exists above the polar front, and the polar front jet is strongest at around 300 hPa. Because the polar front tilts vertically northward with height, the surface polar front is usually located in the latitudes between the two upper westerly jets. However, the two upper jets confluence over the region from the east coast of the Eurasian continent to Japan and the upper westerly jet is restricted to a narrow latitudinal band (roughly 20–40°N) over East Asia. For this region, strong meridional temperature gradients exist also in the lower troposphere around the latitudes of the upper jet stream of the southern branch (see Yoshino, *et al.*, 1985). Therefore, we simply refer the mid-latitude upper westerly jet stream over East Asia to as *the upper westerly jet.*

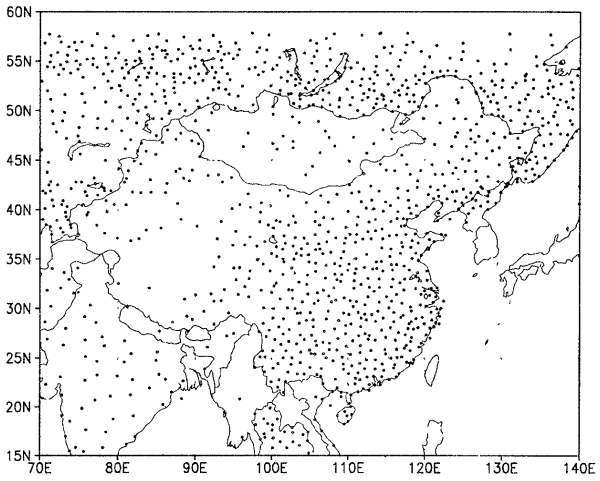

Fig. 1. Spatial distribution of rain gauge observation stations used for producing the grid data.

spheric circulation associated with SPR and to provide a physical explanation why SPR occurs over Central China in spring based on the climatological mean fields.

Section 2 describes data sources and computational procedures. Section 3 re-examines seasonal variations of rainfall over East China. Section 4 examines mean features of large-scale atmospheric circulation in SPR. Section 5 emphasizes changes in large-scale atmospheric circulation associated with the onset of SPR. Section 6 explores the mechanism of SPR or why SPR occurs in spring and over Central China. Section 7 further discusses the results and summarizes main findings.

2. Data and Computational Procedures

Data with two kinds of temporal resolutions were prepared and used. Basically, long-term means of pentad or five-day averaged data were used to describe the seasonal evolutions of rainfall and the associated atmospheric circulation. Monthly mean records were used to examine the year to year variabilities of SPR and several atmospheric indices.

Daily rainfall data of more than 1200 stations from 1980 to 1989 extracted from the Global Daily Summary (GDS) CD-ROM distributed by the National Climatic Data Center (NCDC), NOAA was used to describe the seasonal variation of rainfall over China. The dataset has a very dense spatial distribution (see Fig. 1). To eliminate undesirable spatial inhomogeneity due to orographic effects and/or sampling errors, the station rain gauge observations were interpolated onto $2° \times 2°$ longitude-latitude grid. The bivariate interpolation method, developed by Akima (1978), was used for producing the grid data.

Twice daily, objectively analyzed $2.5° \times 2.5°$ grids of geopotential height (Z), air temperature (T) and horizontal wind ($\boldsymbol{V}$) fields at 850 hPa by ECMWF from 1980 to 1989 were used to explore the associated large scale atmospheric circulation. Specific humidity (q) computed from T and relative humidity was used to examine the moisture field. Relative vorticity (ζ), moisture flux ($q\boldsymbol{V}$) and moisture divergence ($\nabla \cdot q\boldsymbol{V}$) at 850 hPa were also computed from the twice-daily data. All data were compiled to pentad means from the daily or twice-daily datasets to suppress meso- and synoptic-scale variations.

GPCP satellite-derived pentad mean precipitation rates (PR) for the period of 1986–94 was used to demonstrate large-scale precipitation. The data was provided on a $2.5° \times 2.5°$ global grid. A detailed description of this dataset is given by Janowiak and Arkin (1991).

Long-term means for each pentad were calculated by averaging the pentad means of each year. The averaged data were smoothed further by summing up harmonic components 0–6 hence they had still contained some short-term random fluctuations. The number of the harmonic components (NHC) taken for the smoothing was changed between 3 and 15 to examine the influence of NHC or the cut-off frequency of the filter. However, little influence was found for NHC ≥ 6 (not shown). The smoothed data were regarded as the climatological means and will be analyzed. Climatological mean of monthly surface sensible heat flux (SHF) averaged over 1982–1994 from the NCEP/NCAR reanalysis was used to describe the seasonal evolution of spatial distribution of SHF. It was used because only monthly mean data was available currently for the authors' circumstance. The NCEP/NCAR reanalysis is provided on the global $2.5° \times 2.5°$ grid. Since the NCEP/NCAR surface fluxes including SHF are derived solely from the model fields forced by the data assimilation to remain close to the atmosphere, they may strongly depend on the model schemes and may be less reliable than the components from which they were computed, such as temperature and wind. However, comparison of the global mean, zonal mean, and regional distribution of the NCEP/NCAR surface fluxes with observational estimates indicates that the reanalysis climatology agrees with observational climatologies as well as indicating that the different observational climatologies agree with each other (Kalnay *et al.*, 1996). Thus, we only use the climatological mean of SHF. A detailed description of the NCEP/NCAR reanalysis is given by Kalnay *et al.* (1996).

In addition, a 160-station dataset of monthly precipitation prepared by the State Meteorological Bureau of China was used to produce the index of SPR intensity.

Monthly mean sea level pressure (SLP) and T at 850 hPa from the NCEP/NCAR reanalysis for the

period of 1973–1996 were used. Monthly mean SLP from the Compact Disc of the National Meteorological Center Grid Point Data Set: Version II (Gridded NMC analysis for the Northern Hemisphere) was also used because it has a good temporal coverage despite a poor spatial coverage. The dataset, available for 1946–89, is stored on the NMC octagonal grid. The NMC octagonal grid is a 1977 point grid whose points are equally spaced when viewed on a polar stereographic grid, centered on the North Pole with the four corners cut off. The data was interpolated from the NMC octagonal grid into 5°×5° longitude-latitude grid by using a attached program called NMCLAT.FOR. The data is available from 20°N to the North Pole for some longitudes but from 15°N for some longitudes.

In Sections 4 and 5, analyses are based the climatological mean fields of the pentad means. In Section 6, both the pentad mean climatologies and monthly mean data are used.

3. Seasonal variation of rainfall over East China

This section re-examines the seasonal variation of rainfall over East China by using the time-latitude section of rainfall averaged over 110–120°E and identifies several natural seasons including SPR based on the seasonal evolution of rainfall over East China. The spatial patterns of rainfall in SPR and the adjacent natural seasons are also presented.

It is helpful to give the definitions of some regions in China first. The regions of the south of 25°N, 25–30°N, and the north of 35°N of East China (110–120°E) are referred to as South China, Central China, and North China, respectively. Central China and South China are referred to as southern China. Chinese researchers usually refer to the region of the Huai River and the middle and the lower Yangtze River basins (roughly 25–35°N) as Central China. However, in this paper the region of East China between 30°N and 35°N is excluded from Central China because SPR is not remarkable there.

Figure 2 shows the time-latitude section of the rainfall averaged over 110–120°E. The rain-belt experiences a southward movement (S) in mid May and two northward movements (N1 and N2) in mid June and mid July, respectively, from winter to summer. The axis with a weak maximum of rainfall is located between 25°N and 30°N in winter. A remarkable increase of rainfall occurs from the end of February (Pentad 12, 25 Feb–1 Mar, hereafter referred to as P12) and has its maximum at around 28°N in early April (P20, 6–10 Apr). This corresponds to SPR in Central China. At the end of April (P24, 26–30 Apr.), rainfall over Central China begins to decrease while another rain-belt appears at around 24°N. In mid May (P27, 11–15 May)

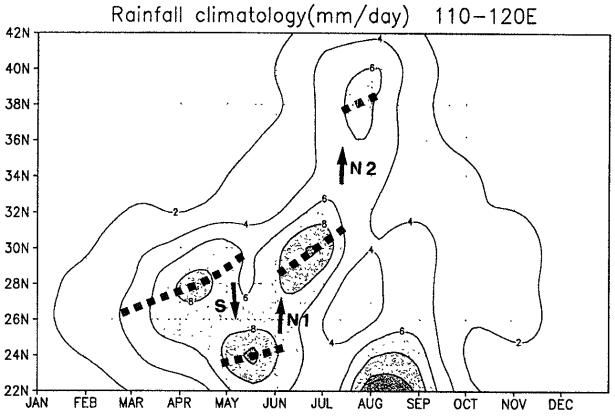

Fig. 2. Time-latitude section of pentad mean precipitation averaged over 110–120°E. Unit is mm · day^{-1}. Heavy broken lines indicate axes of the maximum rainfall in SPR, PMR, Meiyu and the summer rainy period of North China. Arrows with letters S, N1, N2 indicate the southern movement, the first and the second northern movements of the rain-belt, respectively. Sticks on abscissas indicate beginnings of each month throughout the paper.

the main rain-belt shifts to South China completely, while Central China experiences a relative dry spell, which corresponds to the southward movement of the rain-belt (S in Fig. 2). It corresponds to the withdrawal of SPR and the onset of PMR in South China. The two northward jumps (N1 and N2 in Fig. 2) correspond to the onset of Meiyu of Central China in mid June (P33, 10–14 Jun.) and the onset of the summer monsoon rainy period of North China in mid July (P39, 10–14 Jul.), respectively. At the same time, another rain-belt appears in the coastal area of South China, which corresponds to increased visits of typhoons and tropical disturbances. These features derived here generally agree with previous results (*e.g.*, Kao and Hsu, 1962; Xu *et al.*, 1983; Guo, 1985; Lau *et al.*, 1988; Tanaka, 1992).

SPR and the adjacent natural seasons are defined based on the seasonal evolution of rainfall shown in Fig. 2. P1–11 (1 Jan. to 24 Feb.), P12–26 (25 Feb. to 10 May) and P27–32 (11 May to 9 Jun.) are defined as winter, SPR, and PMR, respectively. Although winter starts much earlier than the beginning of the calendar year, for convenience, it is defined here to begin in P1 because our interest is primarily in SPR, and this procedure does not affect the results.

To present the temporal and spatial characteristics of rainfall, the spatial patterns of rainfall in winter, SPR, and PMR are shown in Fig. 3. In winter (Fig. 3a) the rainfall with a weak maximum seen between 25–30°N is restricted mainly to the east

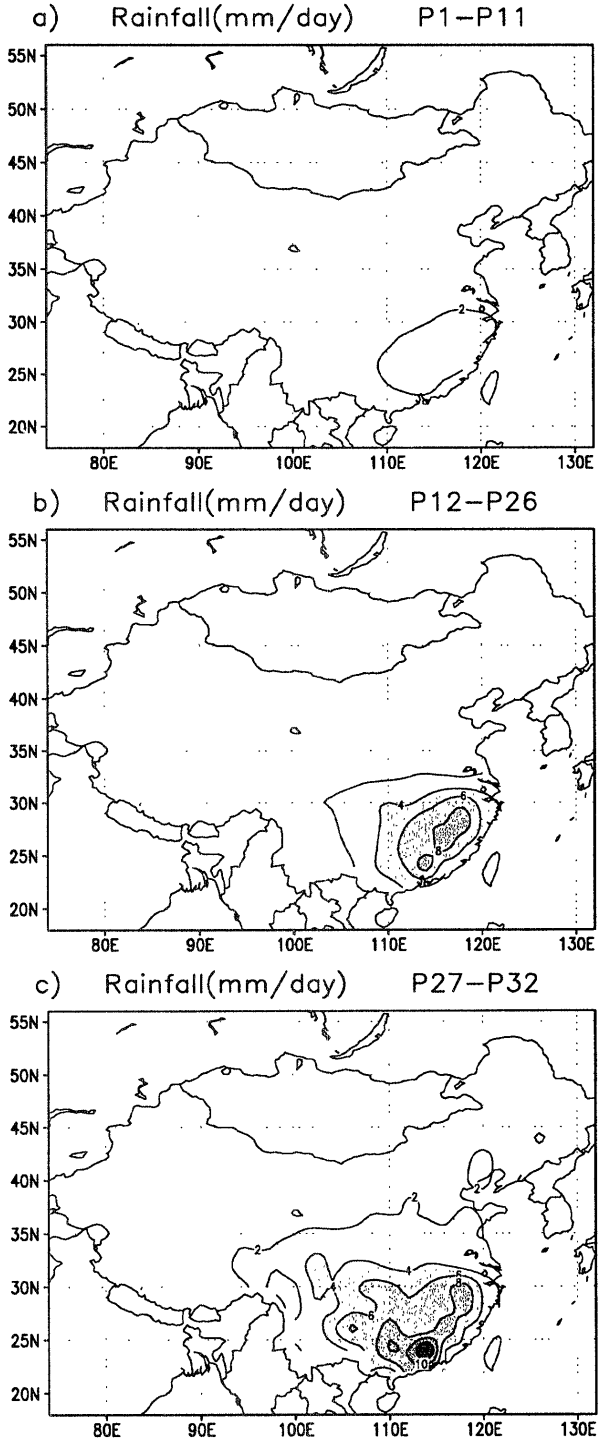

Fig. 3. Pentad mean precipitation in China averaged over winter (a), SPR (b), PMR (c). Contour interval is 2 mm · day^{-1}.

of 110°E. In SPR (Fig. 3b), the spatial pattern is similar to that of winter, but the rainfall increases remarkably. In PMR (Fig. 3c), the axis of the maximum rainfall shifts to the south of 25°N and the area of large rainfall expands westward to 105°E.

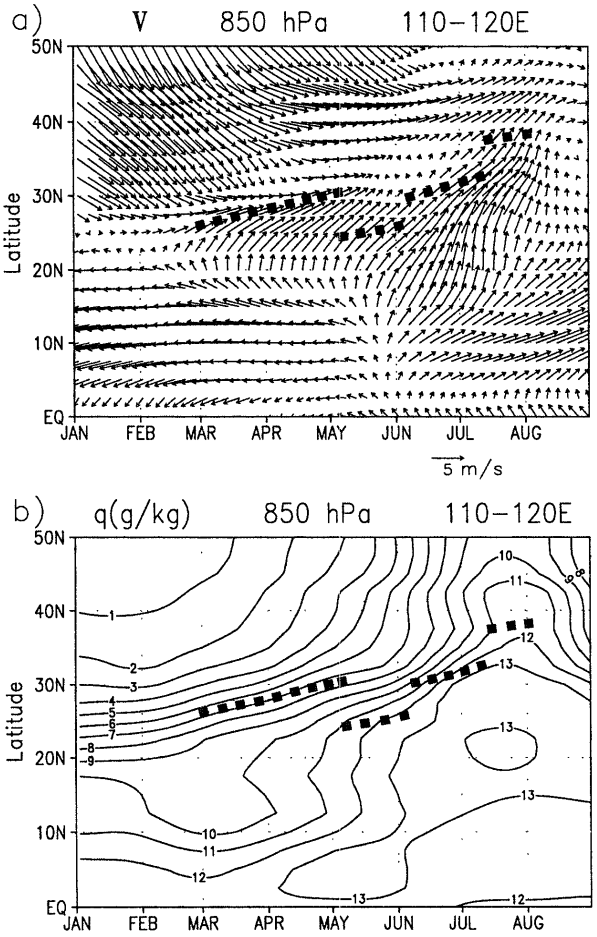

Fig. 4. Time-latitude sections of pentad mean fields of wind vectors (a) and specific humidity (b) at 850 hPa averaged over 110–120°E. Units are m · s^{-1} for wind vectors and g · kg^{-1} for specific humidity. Heavy broken lines indicate axes of maximum rainfall.

4. Mean features of large-scale atmospheric circulation

Before describing the spatial characteristics of the large-scale atmospheric circulation fields associated with SPR, we first show the time evolutions of horizontal wind vector $\boldsymbol{V}$ and moisture (specific humidity) field q at 850 hPa along the longitudes of East China to examine how they correspond to the onset of SPR shown in Fig. 2.

Figure 4a shows the time-latitude variation of $\boldsymbol{V}$ averaged over 110–120°E. At the end of February (P12, 25 Feb.–1 Mar.) southwesterly winds appear at around 27.5°N, which is consistent with the onset of SPR. At the same time, a gradual increase in q at around 25°N (Fig. 4b) is also seen. The onset of SPR seems to correspond to the appearance of southwesterlies and the increase of q in Central China at the end of February.

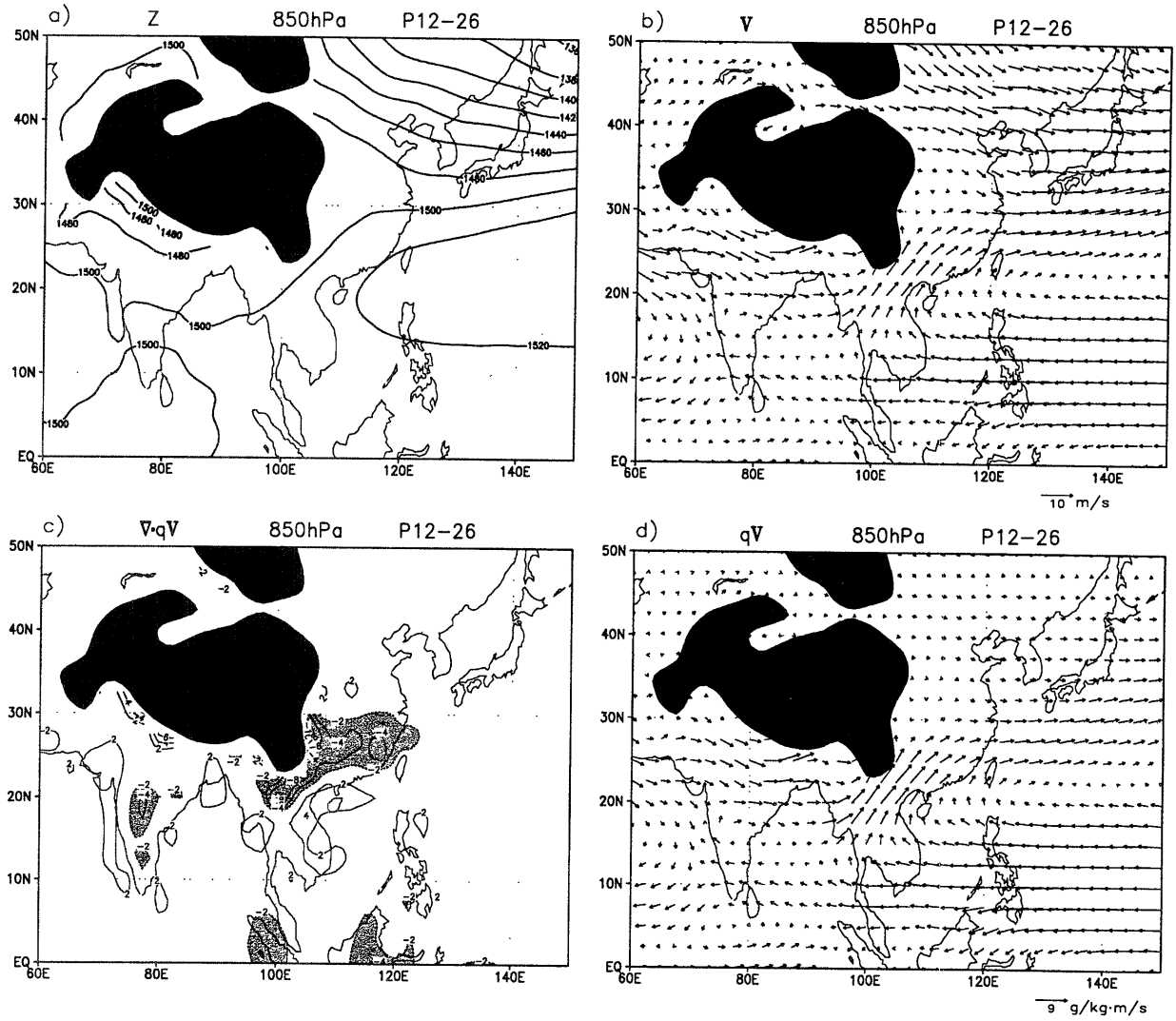

Fig. 5. Mean fields of geopotential height (a), wind vectors (b), moisture divergence (c), and moisture flux (d) at 850 hPa averaged over SPR. Unit is $10^{-6}\mathrm{g}\cdot\mathrm{kg}^{-1}\cdot\mathrm{s}^{-1}$ for moisture divergence. Areas with values of -2 or below are shaded. Black areas on each map indicate regions with mean altitudes of 1500 m or higher throughout the paper.

Next, we examine the mean spatial characteristics of the large-scale atmospheric circulation in SPR. Figure 5 shows the mean fields of Z, $\boldsymbol{V}$, $\nabla \cdot q\boldsymbol{V}$ and $q\boldsymbol{V}$ at 850 hPa in SPR. As shown in the map of Z (Fig. 5a), Central China is located on the northwestern flank of the western North Pacific subtropical high. Low-level southwesterly winds are predominant over southern China, the Indochina Peninsula and southerly winds are observed over the South China Sea (Fig. 5b). It is noteworthy that the southerlies are limited within this region, which is located on the western and northwestern peripheries of the western North Pacific subtropical high. Another feature is that the northwesterlies are evident to the north of 30°N of East Asia. As documented by Bao (1987) the favorable synoptic condition for the persistent rainy weather is that lower- and middle-tropospheric northwesterlies from the northern side and the southwesterlies from southern side confluence over the middle and lower reaches of the Yangtze River to form the stationary front. However, the confluence of the two flows in the climatological mean field in SPR is not clear over the continent, instead, an area of very weak winds exists between the mid-latitude northwesterlies and the subtropical southwesterlies. Perhaps, for the eastern part or the lower Yangtze River basin, the weak winds on the mean map are partially attributed to the cancellation due to the averaging procedure. The western part, or Sichuan Basin may correspond to the so called *dead water region* due to the shelter effect of the Tibetan Plateau (Staff Members, Academia Sinica, 1958).

Southwesterlies are observed over southern China on the day to day synoptic charts when the persistent rainy weather occurs (e.g. Bao, 1987). The

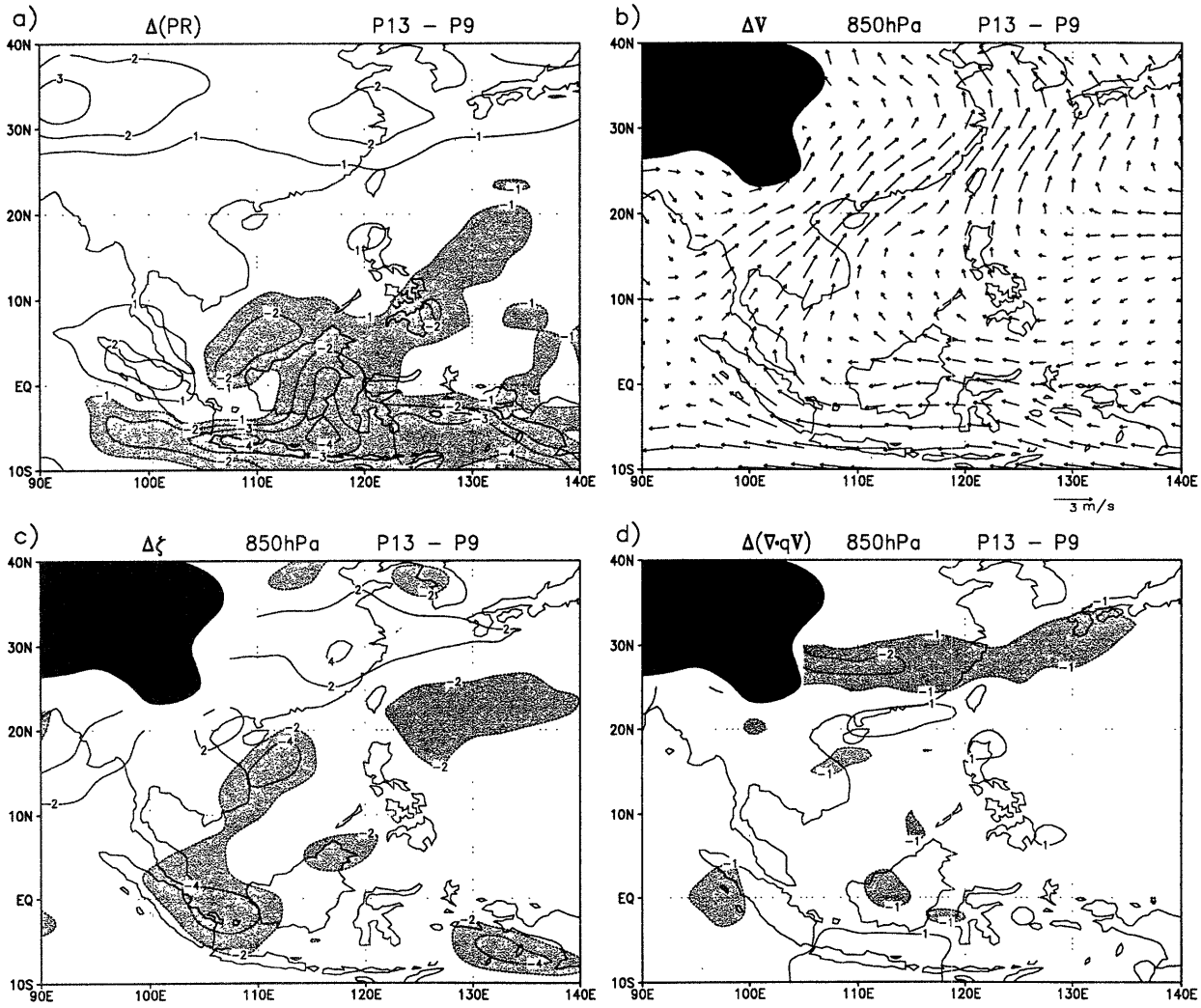

Fig. 6. Differences of fields of GPCP precipitation rate (a), wind vectors (b), relative vorticity (c) and moisture divergence (d) at 850 hPa between two pentads after and before the onset of SPR. Units are mm · day^{-1} for GPCP precipitation rate, 10^{-5}s^{-1} for relative vorticity and 10^{-6}g · kg^{-1} · s^{-1} for moisture divergence. Zero contours are omitted and areas of negative values are shaded.

present study found that southwesterlies are also predominant over southern China in the climatological mean field of $\boldsymbol{V}$ in SPR (Fig. 5b). The southwesterlies on the mean map indicate that southerlies appear more frequently than northerlies in SPR. In addition, it is found that the onset of SPR is consistent with the appearance of the southwesterlies over southern China (Figs. 2, 4a).

A remarkable moisture convergence (negative values) can be found to the south of the middle and lower reaches of the Yangtze River as shown in Fig. 5c. Moisture divergence (positive values) occurs in the region from the Indochina Peninsula to the east of the Philippines. Moisture flux $q\boldsymbol{V}$ suggests that the southwesterly flow on the western flank of the subtropical high seems to mainly contribute to the moisture transport (Fig. 5d). The feature of the $q\boldsymbol{V}$ field derived here is similar to that integrated from the surface to 700 hPa in springs (MAM) of 1981, 1982 by Yatagai and Yasunari (1993).

This section suggests that SPR is related to the low-level southerlies over southern China, which are important for the low-level moisture transport and convergence. The next section will emphasize the changes in the large-scale circulation associated with the onset of SPR.

5. Changes in large-scale atmospheric circulation associated with the onset of SPR

To emphasize the changes in large-scale circulation fields associated with the onset of SPR, the differences of PR, $\boldsymbol{V}$, ζ and $\nabla \cdot q\boldsymbol{V}$ between two pentads before and after the onset are shown in Fig. 6.

A zonally oriented band with increased rainfall is found over the region from Central China to Japan (Fig. 6a). It corresponds with the increase of rain-

fall associated with onset of SPR. The extent of increased rainfall over the region from Central China to the south of Japan suggests that SPR is not a phenomenon due to local orographical effects. Figure 6b shows a strengthening of southwesterlies in the region from the Indochina Peninsula to the east of Taiwan. The area with southwesterly change is located to the south of the band of increased rainfall in Fig. 6a. A southeasterly change is observed to the north of 30°N, which reflects the weakening and retreat of the mid-latitude northwesterlies. Matsumoto (1992) also noted a stepwise northern retreat of the northwesterlies in the mid-latitudes of East Asia in around P14 (7–11 Mar.). He also showed that the low-level northwesterly winds prevail in southern China and northeasterly winds are predominant over around the South China Sea and the Indochina Peninsula in winter. It is interesting that the Indochina Peninsula and the South China Sea correspond to the southern limit of the winter monsoon northerlies (Kao *et al.*, 1962).

A trough line of cyclonic change exists between the areas with weakened northwesterlies and strengthened southwesterlies, and it is consistent with the areas of increased rainfall in Fig. 6a and increased relative vorticity (Fig. 6c). Low-level moisture budget (Fig. 6d) also shows a nearly zonally oriented band of increased moisture convergence located slightly to the south of the axis of increased rainfall over East Asia in Fig. 6a. The northward tilting with height of the polar front surface may explain the slight inconsistency of the locations between the maximum increased rainfall and the maximum increased moisture convergence. The front associated with SPR usually tilts northward vertically with height (Zhu *et al.*, 1992). The warm, moist air from the southern side rises along the front and condensation usually occurs between 850 hPa and 500 hPa. For this reason, the maximum precipitation is usually observed in the north of the position of maximum moisture convergence at 850 hPa.

Another feature is the remarkably decreased rainfall in the tropics, except for the Malay Peninsula and Sumatra, particularly to the south of the equator (Fig. 6a). As shown in Fig. 6b, weakened westerlies or strengthened easterlies are found over the same regions. This result agrees with Matsumoto (1992), who pointed out that there is an abrupt weakening and northern migration of equatorial westerlies in the southern tropics. According to him, it corresponds to the first retreat step of the Australian summer monsoon. Similar results are also reported by Tanaka (1994) who recognized a decrease of high cloud amounts over the Timor Sea at the beginning of March. Therefore, the transition of the maximum of the convective activities from the southern tropics to the northern tropics is also a feature of the large-scale atmospheric circulation around the onset period of SPR. However, it is noteworthy that as a whole the convective activities over the equatorial areas of the Asian-Australian sector is much weaker than in winter.

Further features are the decreased rainfall (Fig. 6a), the anticyclonic wind change (Fig. 6b) and the decreased relative vorticity (Fig. 6c) over east of the Philippines, which suggests a development of an anticyclone. This is consistent with the appearance of the subtropical high in early March noted by Kao and Hsu (1962).

This section suggests that the onset of SPR is related to the cyclonic change in low-level circulation and increased moisture convergence over Central China. Compared with winter, enhanced southwesterly winds on the western flank of the subtropical high of the western North Pacific to east of the Philippines contribute to the increased moisture transport and convergence.

6. Mechanism

In previous sections, we have show that southerlies are remarkable over southern China even in the climatological mean field of $\boldsymbol{V}$ in SPR, and the onset of SPR is closely related to the enhancement of the southerlies over southern China, the Indochina Peninsula and the South China Sea. In this section, we consider the causes for the enhancement of the southerlies in spring.

Figures 5a and 5b indicates that there is an evident westward gradient of the low-level geopotential height over the region from the northern Indochina Peninsula to the western North Pacific to the northeast of the Philippines and the wind vectors are almost parallel to the contours of geopotential height. The meridional component is much dominant than the zonal one for the region 100–110°E, 15–20°N (Fig. 5b). Thus, Figs. 5a and 5b suggests that the low-level southerlies over this region are the geostrophic winds associated with the westward gradient of the low-level geopotential height.

Next, we consider how the east-west gradient of the low-level geopotential height, or the pressure gradient, is formed. To examine the relationship between the low-level temperature and geopotential height fields, the spatial distribution of T at 850 hPa averaged in SPR and its change or the difference of T between two pentads after and before the onset of SPR are shown in Fig. 7. Mean eastward temperature gradient in SPR is most notable along 10–20°N (Fig. 7a). The maximum T appears over the western Indochina Peninsula and the Bay of Bengal. It is noted that the area with large eastward temperature gradient (in Fig. 7a) corresponds to that with the westward gradient of geopotential height Z at 850 hPa in Fig. 5a. In other words, the westward pressure gradient is associated with the eastward temperature gradient over the same region.

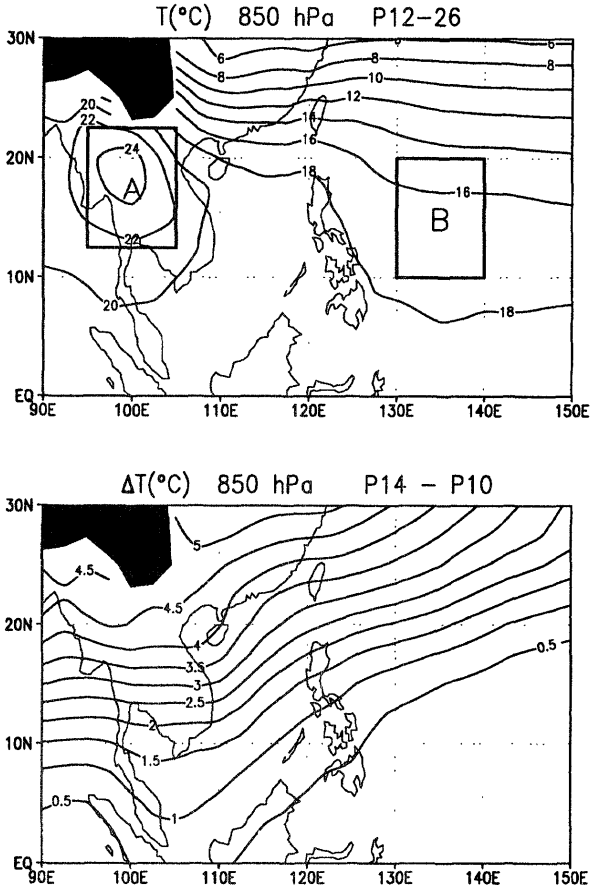

Fig. 7. Temperature at 850 hPa averaged over SPR (a) and the difference of temperature at 850 hPa between two pentads after and before the onset of SPR (b). Unit is °C.

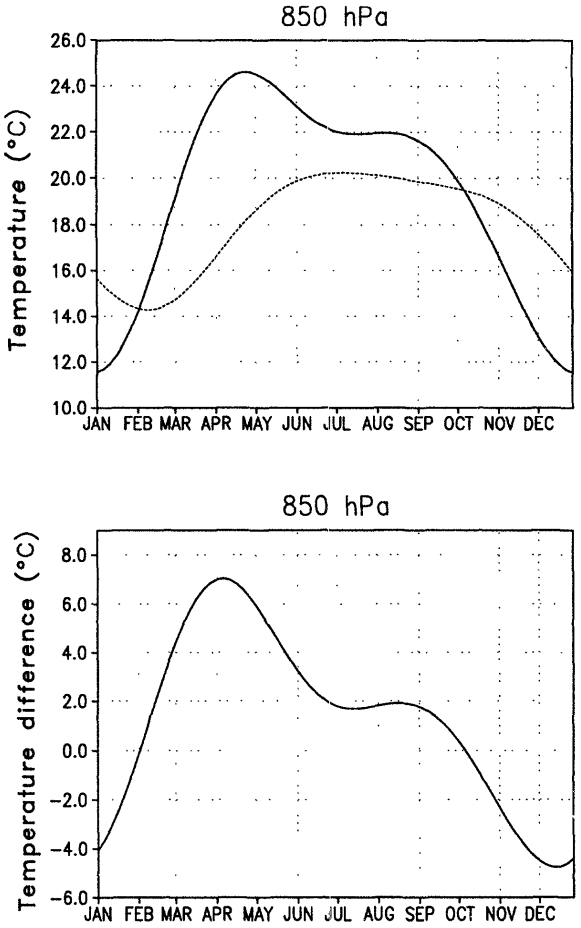

Fig. 8. (a) Seasonal evolutions of pentad mean temperature at 850 hPa averaged over 95–105°E, 12.5–22.5°N (region A in Fig. 7a, solid line) and 130–140°E, 10–20°N (region B in Fig. 7a, dotted line), (b) as in (a) but for difference of temperature between regions A and B.

To further examine when and how this eastward temperature gradient is formed, the seasonal variations of T at 850 hPa over regions A and B in Fig. 7a and the difference of T between the two regions are shown in Fig. 8. The two regions are selected for several reasons. Region A is identical with the area of maximum temperature in SPR. Region B is selected because it is located approximately in the eastern end of area with large zonal temperature gradient and little zonal temperature gradient is found to its north. In addition, since Central China is located nearly in the middle of the two regions longitudinally, the southerly geostrophic wind components between them are supposed to most strongly contribute to SPR.

Figure 8 suggests that the time-lag in the seasonal warming between the two regions is responsible for the eastward temperature gradient in spring. The temperature of region A (solid line) rises sharply from early February to early April, however, that of region B (dotted line) reaches its minimum in early February and rises from late April gradually. The rise of T of region B lags that of region A by more than two months. As a result of the time-lag in the seasonal warming between the two regions, the eastward temperature gradient is most prominent during March and April. It is interesting to note that the temperature gradient reaches its peak in early April, which roughly corresponds to the maximum of SPR rainfall in Fig. 2. The eastward temperature gradient weakens rapidly from May to June.

It is noteworthy that a large temperature rise is also observed in the mid-latitudes of East Asia (Fig. 7b), however, the temperature over the continent is still lower than that over the ocean. The warming in mid-latitudes over East Asia may contribute much to the weakening of the zonal thermal contrast or the zonal pressure gradient, and the consequent retreat and decay of the mid-latitude northerlies. A relatively large meridional temperature gradient or baroclinity still exists over the eastern part of the

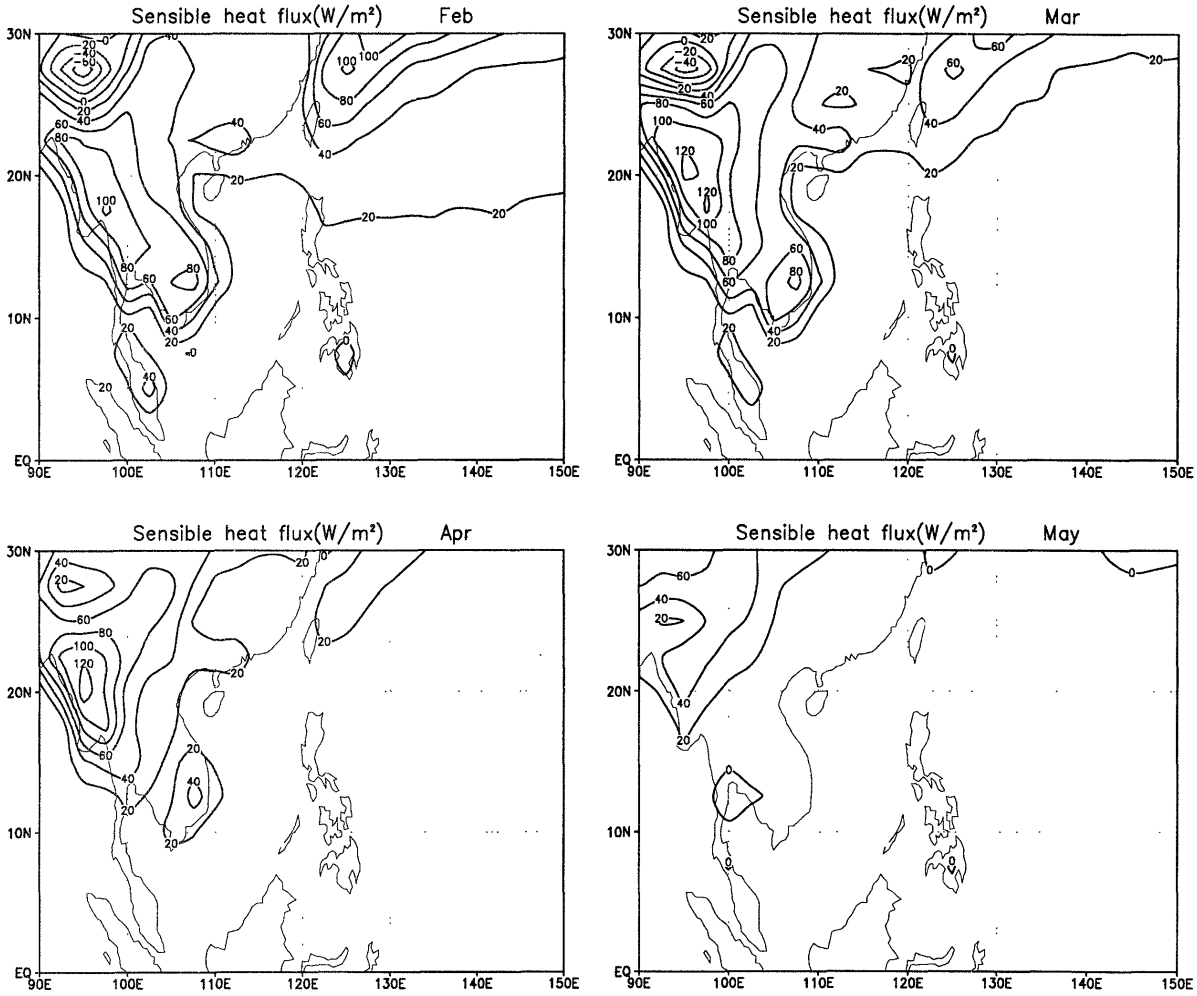

Fig. 9. Spatial distribution of monthly mean sensible heat flux (SHF) from February to May. Unit is $W \cdot m^{-2}$.

continent (Fig. 7a). This agrees with previous results (Kato, 1985, 1987, 1989; Kato and Kodama, 1992; Hirasawa *et al.*, 1995).

To further examine the causes for the time-lag in the seasonal warming between the two regions shown in Fig. 8, climatological means of monthly surface sensible heat flux (SHF) is shown in Fig. 9. SHF over the Indochina Peninsula becomes evident from February. It is most notable in March and April, and the maximum is over the western part. SHF over the oceanic area to the east of the South China Sea is suppressed until May. In February and March another area of large SHF is found from the north of Taiwan to the south of Japan, which corresponds to the Kuroshio current and becomes ill-defined in April. In April, SHF over the southern Indochina Peninsula begins to decrease, and SHF over the whole Indochina Peninsula decreases remarkably in May, particularly for the southern part, where it almost vanishes or even turns into negative over some portion. This is roughly consistent with the relaxation of the temperature difference between the land and oceanic areas shown in Fig. 8b. Figure 9 (right bottom) indicates that the zonal difference of SHF almost disappears in May. This may be related to the enhanced convective activities or increased cloudiness associated with the onset of the Southeast Asian summer monsoon (*e.g.*, He *et al.*, 1987; Hirasawa *et al.*, 1995). It is noteworthy that the low pressure around the Indochina Peninsula and the westward pressure gradient are maintained even after the onset of the Southeast Asian summer monsoon. However, this study indicates that the westward pressure gradient there and the strong heating by SHF over the Indochina Peninsula are already remarkable at least from March, which precedes the onset of the Southeast Asian summer monsoon by more than two months. The change in spatial pattern of SHF from February to May seems to explain well the spatial pattern in SPR (Fig. 7a) and the seasonal evolution of T at 850 hPa (Fig. 8a). These results suggest that the spatial distribution of the low-level temperature around the region from the Indochina Peninsula to the western North Pacific

to the east of the Philippines in spring is likely to be primarily determined by the local SHF. In other words, the eastward temperature gradient is most likely to be explained by the east-west differential heating due to SHF. Increased SHF from the late winter over the Indochina Peninsula primarily accounts for the local quick warming, and the suppressed SHF over the western North Pacific to the east of the Philippines is responsible for the delayed seasonal warming there.

Evidence that suggests the Indochina Peninsula acts as a heat source in spring is found in Yanai *et al.* (1992), though they did not mention it. They estimated the heat budget over the Asian monsoon regions in 1979 from the observational data and noted that the Tibetan Plateau turns from a heat sink to a weak heat source during spring (MAM). However, the most dominant heat source in spring was found over the western part of the Indochina Peninsula (in their Fig. 10). It is noteworthy that their map was the mean for MAM of 1979, thus the heat source over the Tibetan Plateau may mainly reflect the heating in May (*cf.* Fig. 9). On the other hand, Chen and Li (1983) found that the western North Pacific is a heat sink during March and April. These results generally support our analysis.

From this discussion, it is indicated that the eastward temperature/westward pressure gradients account well for the southerlies and consequently for SPR, at least on the seasonal basis. Moreover, the eastward temperature/westward pressure gradients are likely related to the differential heating between the Indochina Peninsula and the western North Pacific to the east of the Philippines. To further confirm the importance of the eastward temperature/westward pressure gradients for SPR and relationships among the year to year variations of SPR intensity, the westward gradient of SLP and the eastward gradient of T at 850 hPa are examined. The mean rainfall in March and April, averaged over 21 rain-gauge observation stations within 25–30°N, 110–120°E, was used as an index of SPR intensity. Difference of SLP, averaged over March and April from NMC between the two regions 20°N, 130–140°E and 15–25°N, 95–105°E, was used as an index of the westward pressure gradient. These two areas are slightly different with regions B and A shown in Fig. 7a because of the limitation of the spatial coverage and resolution of the dataset. However, this index showed a good consistency with the difference of SLP between regions B and A calculated from the NCEP/NCAR reanalysis for the period of 1972–89 (not shown). The difference of T at 850 hPa averaged over March and April between regions A and B was used as an index of the eastward temperature gradient. For comparison, these indices were normalized.

Figure 10 shows the year to year variations of the

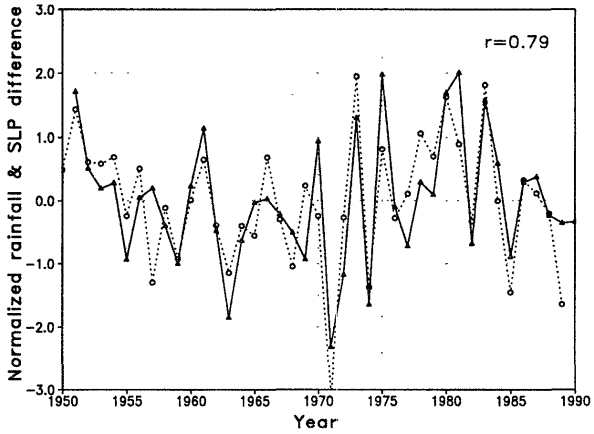

Fig. 10. Year to year variations of normalized SPR index (solid line) and the westward pressure gradient over the Indochina Peninsula through the western Pacific to the east of the Philippines (dotted line). See the text for details.

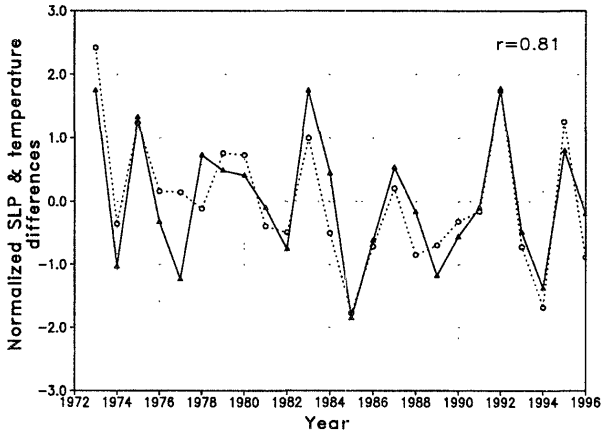

Fig. 11. Same with Fig. 10 but for the westward surface pressure gradient (solid line) and eastward temperature gradient (dotted line) at 850 hPa.

SPR index (solid line) and the westward pressure gradient (dotted line). The fluctuations of the two indices reveal a good correspondence and a strong positive correlation. The correlation coefficient is 0.78, which is much higher than the 99 % significance level (0.41, for 39 samples). The very high correlation indicates that a close relation between SPR and the westward pressure gradient exists also on the interannual time-scale. Figure 11 shows the year-to-year variations of the indices of the westward pressure gradient (solid line) and the eastward temperature gradient (dotted line). The two series very nearly parallel to each other. The correlation coefficient is 0.81, which is also much higher than the 99 % significance level (0.52 for 24 samples). This very high correlation indicates a close

relationship between the eastward temperature and the westward pressure gradients on the interannual time-scale. The close relationship among SPR and the eastward temperature/westward pressure gradients on the interannual time-scale strongly suggests that the interannual variation in the east-west thermal contrast between the Indochina Peninsula and the western North Pacific to the east of the Philippines is responsible for the interannual fluctuations of SPR.

This section indicates that SPR is closely related to the low-level eastward temperature/westward pressure gradients on both the seasonal and interannual bases.

7. Discussion and concluding remarks

The atmospheric circulation in spring has been considered as the winter monsoon circulation regime (*e.g.*, Yeh *et al.*, 1959; Yoshino, 1965, 1966) because the maximum axis of the upper westerly jet is located to the south of the Tibetan Plateau. However, our results indicate that the low-level southerlies have appeared over southern China, the Indochina Peninsula and the South China Sea in SPR. In this sense, the atmospheric circulation in SPR is obviously different from that in winter.

The atmospheric circulation in SPR is completely different from that in Meiyu. In SPR the low-level southerlies are limited in the region of southern China, the Indochina Peninsula and the South China Sea (in Fig. 5b). On the other hand, after the onset of Meiyu, fully developed low-level southwesterlies prevail over regions from the broad Indian Ocean extending through the Bay of Bengal, the Indochina Peninsula to Central China and Japan to merge with the southwesterlies on the northwestern flank of the western North Pacific subtropical high (*e.g.*, Murakami, 1959; Tao and Chen, 1987; Matsumoto, 1992). In addition, low-level cross-equatorial currents over the maritime continents also influence Central China during Meiyu season (*e.g.*, Tao and Chen, 1987). Furthermore, as noted by many researchers (*e.g.*, Yeh *et al.*, 1959; Yoshino, 1965, 1966) the atmospheric circulation in the middle and upper troposphere is essentially the same with that in winter except for the weakening of the southern branch of the mid-latitude upper westerly jet (Staff Members, Academia Sinica, 1957). After Meiyu onset, associated with establishment of the upper Tibetan anticyclone the maximum of the upper westerly jet moves to the northern side of the Tibetan Plateau and easterlies appear on the southern side (*e.g.*, Dao and Chen, 1957; Yeh *et al.*, 1959). Therefore, SPR has completely different horizontal and vertical structures from Meiyu.

SPR is a transitional stage from the northern winter/southern summer monsoon circulation regime to the northern summer/southern winter monsoon circulation regime. The northwesterlies over East Asia associated with Siberian high are also much weaker than in winter and have retreated to the north of 30°N (Fig. 5b). This result agrees with Matsumoto (1992). During this period, the Tibetan Plateau changes from a weak heat sink to a weak heat source but northern China still acts as a heat sink (Yanai *et al.*, 1992). At the same time, convective activities over northern Australia and the marinetime continents are much weaker than in northern winter (in Fig. 6a). It corresponds to the first retreat step of the Australian and Indonesian summer monsoon noted by Matsumoto (1992). A similar result is also noted by Tanaka (1994). The decayed convective activities imply that the heat source over the maritime continents and northern Australia is much weaker than in northern winter. This stage also precedes the onsets of the summer monsoon over regions of the Bay of Bengal, the Indochina Peninsula, the South China Sea and the western North Pacific around the Philippines, which act as the major heat sources in summer (Chen and Li, 1983; Yanai *et al.*, 1992). Kato (1989) also suggested that there are no wide heat sources to the west of the subtropical high of western North Pacific before the onset of the Southeast Asian summer monsoon. These facts suggest that there are no huge heat source in SPR. The low-level eastward temperature/westward pressure gradients over region from the Indochina Peninsula to the western North Pacific to the east of the Philippines associated with the local differential heating by SHF play the primary role on the low-level circulation over the Indochina Peninsula, the South China Sea and southern China for lack of huge heat sources. Therefore, the differential heating during spring is essential for SPR. The very high correlations among the year to year fluctuations of SPR and the eastward temperature/westward pressure gradients strongly support this consideration.

Main findings of the current study are as follows.

1. Low-level southwesterlies to the south of the middle and lower reaches of the Yangtze River (southern China) are responsible for SPR. Low-level southwesterlies are identified over southern China in the climatological mean wind field in SPR, and the appearance of the southwesterlies at the end of February is consistent with the onset of SPR. The southerlies are limited to southern China, the Indochina Peninsula and the South China Sea, which are important for the moisture transport to Central China and the moisture convergence there.

2. Seasonal evolutions of low-level temperature, geopotential height and wind fields suggest that the low-level southerlies over southern China, the Indochina Peninsula and the South China Sea in SPR are attributed to the westward pres-

sure gradient associated with the eastward temperature gradient around the region from the Indochina Peninsula to the western North Pacific to east of the Philippines. The southerlies are the geostrophic winds associated with the westward pressure gradient. The eastward temperature/westward pressure gradients are most evident in March and April, and they are a result of the time-lag in the seasonal warming between the Indochina Peninsula and the western North Pacific to the east of the Philippines. In addition, the coincidences of spatial distributions and seasonal evolutions from February through May between the low-level temperature and the surface sensible heat flux (SHF) suggest that the differential heating due to SHF between the two regions is likely responsible for the east-west thermal contrast.

3. Much higher correlations than the 99 % significance level among the year to year fluctuations of SPR and the eastward temperature/westward pressure gradients over the region from the Indochina Peninsula to the western North Pacific to the east of the Philippines are identified. The close relationship among SPR and the eastward temperature/westward pressure gradients on both the seasonal and interannual bases strongly suggests that the east-west thermal contrast in spring between the Indochina Peninsula and the western North Pacific to the east of the Philippines plays the primary role on SPR.

Several problems remain to be solved. This study presented the large-scale features of the atmospheric circulation associated with SPR based on the climatological means and provided a physical explanation of the rainy season in Central China climatologically. However, the dynamical mechanism for the maintenance of the rainy weather for 5–7 days and occasionally for weeks (*e.g.*, Bao, 1987) remains unsolved. It is found that the large-scale atmospheric circulation in the lower latitudes play a primary role on SPR. However, basically SPR is a phenomenon in the mid-latitude baroclinic zone (Kato and Kodama, 1992; Hirasawa *et al.*, 1995). Actually, a relatively strong meridional temperature gradient exists in SPR (Fig. 7a; also see Kato, 1985, 1987, 1989). The atmospheric circulation in the higher latitudes may also influence SPR. This point should be examined.

Acknowledgments

The authors appreciate Profs. F. Kimura, A. Kitoh and Dr. H.L. Tanaka, all of the Institute of Geoscience, University of Tsukuba for their valuable comments. The authors are grateful to Dr. Ryuichi Kawamura of the National Research Institute for Earth Science and Disaster Prevention, for his continuous discussion and many suggestions. The first author would like to express his appreciation to Prof. Kazuo Kotoda of Faculty of Regional Development Studies, Toyo University, for his encouragement and support when he was the director of Environmental Research Center, University of Tsukuba. The authors also appreciate Prof. T. Murakami, an emeritus professor at the University of Hawaii and Dr. J. Matsumoto of Department of Geography, Tokyo University for their interest and discussion. The authors also acknowledge the two anonymous reviewers; their valuable comments greatly improved the clarity of this paper. The authors thank Mr. Lei Gao and Ms. Ailikun for partial computation assistance.

NCAR/NCEP reanalysis data were provided through the NOAA Climate Diagnostics Center (http://www.cdc.noaa.gov/). The Global Daily Summary (GDS) data was produced by the NOAA Climate Prediction Center, and distributed on CD-ROM by the National Climatic Data Center (NCDC), NOAA. NMC gridded analysis for the Northern Hemisphere was prepared and maintained by the Data Support Section, Scientific Computing Division, National Center for Atmospheric Research (NCAR). NCAR is operated by the University Corporation for Atmospheric Research and is sponsored by the National Science Foundation. GPCP (Global Precipitation Climatology Project) dataset was prepared and maintained by the Data Support Section, Scientific Computing Division, NCAR. The data was originally provided by J. Janowiak, NOAA and G. Huffman, NASA. The monthly mean precipitation data of China was compiled by the State Meteorological Administration of China. This study was partially supported by Grant-In-Aid from the Ministry of Education (No. 09227208).

All the figures were drawn with GrADS, a free software developed by Brian E. Doty, Center for Ocean-Land-Atmosphere Interactions, Department of Meteorology, University of Maryland. Some GrADS scripts written by Mike Fiorino of Lawrence Livermore National Laboratory were also helpful.

The first author also thanks the staffs of Environment Research Center, University of Tsukuba, for much indirect support.

References

Akima, H., 1978: A method of bivariate interpolation and smooth surface fitting for irregularly distributed data points. *ACM Transactions on Mathematical Software*, **4**, 148–159.

Bao, C.-L., Ed., 1987: *Synoptic meteorology in China.* China Ocean Press, Beijing (Overseas distributed by Springer-Verlag, Berilin, Heidelberg, New York, Tokyo), 269pp.

Chen, L.-X. and W.-L. Li, 1983: The structure of monthly atmospheric heat sources in the monsoon region of Asia. *Proc. Symp. on the Summer Monsoon in South East Asia, 1982 Kunming, China*, 86–101 (in Chinese with English abstract), People's Press of Yunnan Province, Kunming, China.

Dao, S.-Y. and L.-S. Chen, 1957: The structure of general circulation over continent of Asia in summer. *75th Ann. Vol. J. Meteor. Soc. Japan*, 215–229.

Guo, Q., 1985: The variations of summer monsoon in East Asia and the rainfall over China. *J. Tropical Meteor.*, **1**, 44–52 (in Chinese with English abstract).

He, H., J. McGinnis, Z. Song and M. Yanai, 1987: Onset of the Asian summer monsoon in 1979 and the effect of the Tibetan Plateau. *Mon. Wea. Rev.*, **115**, 1966–1995.

Hirasawa, N., K. Kato and T. Takeda, 1995: Abrupt change in the characteristics of the cloud zone in subtropical East Asia around the middle of May. *J. Meteor. Soc. Japan*, **73**, 221–239.

Hsu, S.-Y. and Y.-H. Kao, 1962: East Asia monsoon and seasons. Y.-H. Kao, Ed., *Some Problems on Monsoons in East Asia*, Science Press, Beijing, 88–103 (in Chinese).

Janowiak, J. and P.A. Arkin, 1991: Rainfall variations in the tropics during 1986–1989, as estimated from observations of cloud-top temperature. *J. Geophys. Res.*, **96**, 3359–3373.

Kalnay, E., M. Kanamitsu, R. Kistler, W. Collins, D. Deaven, L. Gandin, M. Iredell, S. Saha, G. White, J. Woollen, Y. Zhu, M. Chelliah, W. Ebisuzaki, W. Higgins, J. Janowiak, K.C. Mo, C. Ropelewski, J. Wang, A. Leetmaa, R. Reynolds, R. Jenne and D. Joseph, 1996: The NCEP/NCAR 40-year reanalysis project. *Bull. Amer. Meteor. Soc.*, **77**, 437–471.

Kao, Y.-H. and S.-Y. Hsu, 1962: Advance and retreat of East Asian monsoons and the beginning and ending of rainy periods. Y.-H. Kao, Ed., *Some Problems on Monsoons in East Asia*, Science Press, Beijing, 78–87 (in Chinese).

Kao, Y.-H., S.-Y. Hsu, Q.-Y. Guo and M.-L. Zang, 1962: Monsoon regions and regional climate in China. Y.-H. Kao, Ed., *Some Problems on Monsoons in East Asia*, Science Press, Beijing, 49–63 (in Chinese).

Kato, K., 1985: On the abrupt change in the structure of the Baiu front over China continent in late May 1979. *J. Meteor. Soc. Japan*, **63**, 20–36.

Kato, K., 1987: Airmass transformation over the semi-arid region around North China and abrupt change in the structure of the Baiu front in early summer. *J. Meteor. Soc. Japan*, **65**, 737–750.

Kato, K., 1989: Seasonal transition of the lower-level circulation systems around the Baiu front in China in 1979 and its relation to the Northern Summer Monsoon. *J. Meteor. Soc. Japan*, **67**, 249–265.

Kato, K. and Y. Kodama, 1992: Formation of the quasi-stationary Baiu front to the south of the Japan Islands in early May of 1979. *J. Meteor. Soc. Japan*, **70**, 631–647.

Lau, K.-M., G. Yang and S. Shen, 1988: Seasonal and intraseasonal climatology of summer monsoon rainfall over East Asia. *Mon. Wea. Rev.*, **116**, 18–37.

Matsumoto, J., 1989: The seasonal changes of tropical cloud distribution as revealed from 5-day mean outgoing longwave radiation. *Bulletin of the Department of Geography, University of Tokyo*, **21**, 19–35.

Matsumoto, J., 1990: The seasonal changes of wind fields in the global tropics. *Geographical Review of Japan*, **63B**, 156–178.

Matsumoto, J., 1992: The seasonal changes in Asian and Australian monsoon regions. *J. Meteorol. Soc. Japan*, **70**, 257–273.

Murakami, T., 1959: The general circulation and water-vapor balance over the Far East during the rainy season. *Geophys. Mag.*, **29**, 131–171.

Staff Members, Academia Sinica, 1957: On the general circulation over Eastern Asia (I). *Tellus*, **9**, 432–446.

Staff Members, Academia Sinica, 1958: On the general circulation over Eastern Asia (II). *Tellus*, **10**, 58–75.

Tanaka, M., 1992: Intraseasonal oscillation and the onset and retreat dates of the summer monsoon over East, Southeast Asia and the western Pacific region using GMS high cloud amount data. *J. Meteor. Soc. Japan*, **70**, 613–629.

Tanaka, M., 1994: The onset and retreat dates of the Austral summer monsoon over Indonesia, Australia and New Guinea. *J. Meteor. Soc. Japan*, **72**, 255–267.

Tao, S. and L. Chen, 1987: A review of recent research on the East Asian summer monsoon in China. C.-P. Chang and T. Krishnamurti, Eds., *Monsoon meteorology*, Oxford University Press, Inc, New York, p60–92.

Xu, G., M. Li and Z. Zhang, 1983: Seasonal variation of the rain-belts in China. *Sci. Atmos. Sinica*, **7**, 312–318 (in Chinese with English abstract).

Yanai, M., C. Li and Z. Song, 1992: Seasonal heating of the Tibetan Plateau and its effects on the evolution of the Asian summer monsoon. *J. Meteor. Soc. Japan*, **70**, 319–351.

Yatagai, A. and T. Yasunari, 1993: The precipitation and water vapor transport over around the arid and semi-arid regions of China. *Proceedings of the Japan-China International Symposium on the Study of the Mechanism of Desertification*, 349–355.

Yeh, T.-C., S.-Y. Dao and M.-T. Li, 1959: The abrupt change of circulation over the Northern Hemisphere during June and October. B. Bolin, Ed., *The Atmosphere and the Sea in Motion, Rossby Memorial*, The Rockefeller Institute Press, New York, 249–267.

Yoshino, M., 1965: Four stages of the rainy season in early summer over East Asia (Part I). *J. Meteor. Soc. Japan*, **43**, 231–245.

Yoshino, M., 1966: Four stages of the rainy season in early summer over East Asia (Part II). *J. Meteor. Soc. Japan*, **44**, 209–217.

Yoshino, M., T. Asai, T. Kawamura, H. Shitara, T. Nitta and I. Maejima, Eds., 1985: *Glossary of Climatology and Meteorology.* Ninomiyashoten, Tokyo, Japan, 742pp (in Japanese).

Zhu, Q.-G., J.-R. Lin, S.-W. Shou and D.-S. Tang, Eds., 1992: *Principle and Method of Synoptic Meteorology.* Meteorological Publishing, Beijing, China, revised edition, 914pp (in Chinese).

華中における春の長雨の気候学的特徴とそのメカニズム

田　少奮
（筑波大学水理実験センター）
安成哲三
（筑波大学地球科学系）

本研究は、主に降水量の観測データおよび850 hPaにおける等圧面高度、風、気温、相対湿度の客観解析格子点データの5日平均の平年値を用いて、華中における春の長雨(SPR)に関連する大規模な循環場の特徴を調べた。また、SPRの気候学的な成因の物理的解釈を提案した。

SPRは2月の終わりに開始し、5月の始めまで続く。SPR期の下層の平均場において揚子江中下流域以南の地域(中国南部)で南西の風が卓越している。この下層の南寄りの風は中国南部、インドシナ半島と南シナ海に限られている。中国南部における下層の南寄りの風の出現はSPRの開始とよく対応しており、華中への水蒸気輸送とそこでの水蒸気収束に大きく寄与している。したがって、この下層の南寄りの風はSPRに重要である。

850 hPaにおける等圧面高度、気温、風の場の季節進行から、下層の南寄りの風は、インドシナ半島からフィリピン東方の西部北太平洋付近にかけての下層の東向きの気温傾度に関連する西向きの気圧傾度に対する地衡風平衡の結果であることが分かった。この東向きの気温/西向きの気圧傾度は3月と4月に最大であり、インドシナ半島付近とフィリピン東方の西部北太平洋での昇温のずれによって生じるものである。インドシナ半島からフィリピン東方の西部北太平洋にかけての下層の気温と地表からの顕熱フラックスの季節変化が似ていることから、2月から4月におけるインドシナ半島付近の地表からの顕熱フラックスによる加熱が東西の熱的コントラストの主な原因であると考えられる。

年々変動においても、SPRと上に述べた東向きの気温/西向きの気圧傾度の間に99 %有意水準を超える非常に高い相関が確認された。季節変化、経年変動におけるSPRと東向きの気温傾度/西向きの気圧傾度との間の密接な関係はインドシナ半島付近とフィリピン東方の西部北太平洋の間の東西の熱的コントラストがSPRにとって本質的であることを強く示唆している。